Biochimica et Biophysica Acta 1818 (2012) 2975–2981

Contents lists available at SciVerse ScienceDirect

Biochimica et Biophysica Acta

journal homepage: www.elsevier.com/locate/bbamem

Binding and reorientation of melittin in a POPC bilayer: Computer simulations

Sheeba J. Irudayam, Max L. Berkowitz *

Department of Chemistry, University of North Carolina at Chapel Hill, 131 South Road, Chapel Hill, North Carolina, NC 27599, USA

ARTICLE INFO

Article history:
Received 11 June 2012
Received in revised form 26 July 2012
Accepted 27 July 2012
Available online 2 August 2012

Keywords:
Antimicrobial peptides
Lipid bilayers
Pores in bilayers
Molecular dynamics simulations
Melittin

ABSTRACT

We performed, using an all-atom force field, molecular dynamics computer simulations to study the binding of melittin to the POPC bilayer and its subsequent reorientation in this bilayer. The binding process involves a simultaneous folding and adsorption of the peptide to the bilayer, followed by the creation of a "U shaped" conformation. The reorientation of melittin from the parallel to the perpendicular conformation requires charged residues to cross the hydrophobic core of the bilayer. This is accomplished by a creation of defects in the bilayer that are filled out with water. The defects are caused by peptide charged residues dragging the lipid headgroup atoms along with them, as they reorient. With increased concentration of melittin water defects form stable pores; this makes it easier for the peptide N-terminus to reorient. Our results complement experimental and computational observations of the melittin/lipid bilayer interaction.

1. Introduction

Melittin is one of the widely studied antimicrobial peptides, but we are still lacking a molecular level understanding of the mechanism of its interaction with lipid bilayers. It is believed [1] that the antimicrobial action of melittin involves forming a toroidal pore in the bacterial membrane that eventually leads to the cell death. For melittin to insert into a pore and become a part of this pore it needs to be in a transmembrane orientation. However, the mechanism by which melittin reaches this transmembrane orientation remains ambiguous. For example, Bogaart et al. [2] suggested that melittin binding parallel to membrane surface and a direct perpendicular insertion of melittin into a membrane are two competing mechanisms. Most of the research [1,3,4] indicates that melittin binds first to a lipid bilayer and then reorients into a transmembrane conformation. According to Huang et al. [1], at low peptide concentration melittin mostly adopts a parallel conformation; with the increase in peptide concentration the fraction of peptides in the transmembrane orientation increases. Melittin is not the only peptide that is believed to create toroidal pores in membranes; another well-studied peptide also believed to create toroidal pores is magainin. Nevertheless, the details of pore creation by melittin and magainin differ, as was clearly demonstrated by recent experiments that monitored dye efflux from giant unilamellar vesicles ruptured by peptides [3]. When the peptide was magainin, the complete dye release from many vesicles occurred during a short time, and therefore the process got the name "all-or-none". For melittin the release is gradual and consequently the process was named "graded". This clearly indicates that the molecular level architecture of the pores through which the dye release occurs is quite different in cases of melittin and magainin.

Computer simulations play an important role in providing detailed molecular description of many biological phenomena, description that is often hard, if not impossible, to get from the experiment. Therefore simulations were also employed to study interactions of antimicrobial peptides with membranes, including simulations on systems containing melittin interacting with lipid bilayers [5]. Detailed, all-atom force field simulations of bilayer/melittin system showed that a) indeed, as it was suggested, to create a pore the concentration of melittin has to be above certain critical concentration, and b) melittin induced toroidal pores do not have a regular shape and peptides do not line up the walls of the pores [5]. Based on the results from these simulations a new model for a pore in membrane due to the presence of a peptide was suggested by Marrink and his coworkers, a disordered toroidal pore [5]. But detailed molecular dynamics simulations cannot explore large time intervals over which a regular toroidal pore may be created. To circumvent this problem toroidal pores with a regular arrangement of melittin peptides were prepared as initial structures and simulations that studied details of such pores were performed [6–9].

Since all-atom simulations are still limited in the scope of time periods and spatial domains they can cover, simulations that employ coarse-grained force fields are used to study peptide-membrane interactions. Especially useful results are obtained from the studies that use a force field called MARTINI [10,11], and our group also used it to study spontaneous pore creation by melittin and by magainin peptides [12]. In our previous coarse-grained simulations it was observed that magainin created large pores, while melittin smaller pores, thus connecting the pore structures to the character of dye efflux. It was also observed that some of the melittin peptides were in a "U-shaped conformation", due to the presence of PRO residue that allows bending

* Corresponding author. Tel.: +1 919 962 1218; fax: +1 919 962 2388.
E-mail addresses: isheeba@email.unc.edu (S.J. Irudayam), maxb@unc.edu (M.L. Berkowitz).

0005-2736/$ – see front matter © 2012 Elsevier B.V. All rights reserved.
http://dx.doi.org/10.1016/j.bbamem.2012.07.026

of the peptide around its middle at the location of this residue. This also allows both charged termini regions to be solvated by the polar headgroups of the lipids, while the hydrophobic region in the middle of the peptide could penetrate into the hydrophobic region of the bilayer. These "U-shaped" melittin peptides were also observed in simulations [12] to be located in the pores, possibly blocking, or slowing down the efflux through the pores. While simulations with MARTINI produced many successes, it has its shortcomings, and it is important to understand if the "U-shaped" conformation observed in coarse-grained simulations is not an artifact of the force field.

Since most of the research points out that melittin creates pores by first adsorbing to the membrane surface and then, after reaching critical concentration, may create pores by reorienting and acquiring a transmembrane configuration, we want to study this mechanism in more detail. We also want to understand if the mechanism of peptide reorientation from parallel to transmembrane orientation changes when the concentration of melittin peptides changes from low (pre-critical concentration of P/L = 1/128, one peptide per 128 lipids in our simulation system) to higher (post-critical concentration of P/L = 4/128).

In this paper we describe results from all atom simulations performed to study binding and reorientation of melittin in a POPC bilayer using molecular dynamics simulations with the umbrella sampling technique. We also use regular molecular dynamics simulations to study further structural details, if needed. Umbrella sampling allows getting quantitative information on free energies when the coordinates that are orthogonal to the coordinate of interest reach fast equilibrium. This may not be the case when we want to study the approach of a peptide to a membrane surface and, therefore, more constrains in the simulations need to be imposed. As a result, it is more difficult to compare quantitatively the experimental results and simulations. However, the trajectories obtained from umbrella sampling simulations offer valuable information on the behavior of the system along the reaction coordinate. In this work we focus more on this qualitative aspect of the umbrella sampling simulations and combine it with the observations from regular MD to understand the binding and reorientation of melittin.

2. Methods

We performed different simulations to understand different stages of melittin interaction with the lipid bilayer; I) its initial adsorption to the bilayer surface in a parallel to the surface conformation, followed up by II) reorientation of the peptide from a parallel to a transmembrane conformation.

I a) Binding of melittin from water to the bilayer: umbrella sampling simulations. To understand the thermodynamics of melittin binding to the bilayer one needs to find the binding free energy. This requires very large calculations to sample properly all configurations of the peptide. In case when the peptide is not flexible and can be considered to be a rigid rod, the calculations can be done for a set of different angles between the rod and the bilayer. Finally these free energies, each calculated for a given angle, can be properly summed up [13]. Since melittin is not a rigid rod, this strategy will not work. Moreover, it is understood that melittin undergoes structural transition as it approaches a bilayer: while far away from the bilayer it is a coil, melittin transforms into a helix when adsorbed to a lipid bilayer surface. Given all the difficulty in obtaining accurate quantitative thermodynamic information from simulations with melittin, we decided to get a feeling of thermodynamics of the melittin adsorption and also investigate if indeed structural transformations in melittin occur as a function of distance from the bilayer. Therefore, we performed umbrella sampling calculations with melittin exploring a subset of its conformations: when melittin approaches the bilayer in a parallel orientation. For this purpose we placed the crystal structure of melittin parallel to bilayer with its center of mass at 13 equidistant positions between 5.0 and 2.6 nm away from the bilayer center, along the z-direction. The force constant for the umbrella potential was 200 kJ/mol. To restrain the orientations of the peptide, in addition to restraining its center of mass, the center of mass of helix "a" (residues 1–14), and the center of mass of helix "b" (residues 15–26) were also restrained to explore the same distances from the bilayer center as the center of mass of the whole peptide.

I b) Regular MD simulation of bound melittin: To validate the observations from the umbrella sampling simulations, we performed a regular MD simulation placing two melittin peptides (one on each leaflet), just above the headgroup region (~3 nm from the bilayer center). We used two peptides to improve the sampling. From the umbrella sampling simulations for binding it was observed that as the peptide approached the bilayer it had an orientation such that its hydrophobic side faced water and the hydrophilic side faced the lipid headgroups. Therefore, while setting up the system for the regular MD runs, the two peptides were oriented such that their hydrophilic sides were facing the bilayer headgroup region and the hydrophobic sides faced water. A 200 ns run of this system was performed at constant pressure and the dynamics of the peptides was monitored.

II a) The reorientation of melittin from a parallel conformation to a transmembrane conformation: The reorientation of a melittin molecule from the parallel to the perpendicular orientation at P/L = 1/128 was studied by pulling the center of mass of the first three residues of the N-terminus of melittin. These residues were pulled from the upper to the lower leaflet of the bilayer. For simplicity, the first three residues of the N-terminus of melittin will be referred to as the pulling group. The pulling group was placed at 15 distances from 3.4 nm to 0.6 nm from the center of the phosphate groups in the lower leaflet with an interval of 0.2 nm and umbrella potential of 200 kJ/mol. However with this distribution of windows, certain regions along the reaction coordinate were not sampled since the force constant was not large enough to hold the pulling group at the window position, therefore to enable sufficient overlap between the windows we had to add four additional windows at 1.3 nm, 1.4 nm, 1.9 nm and 2.1 nm. These windows had a force constant of 1000 kJ/mol.

The initial structures for the umbrella sampling simulations were setup by placing the crystal structure of the peptide with its pulling group at the window position, minimizing and equilibrating the system. Since generating the initial structures involves placing the peptide into the hydrophobic core of the bilayer, this was done by placing the peptide in a preformed pore of a bilayer downloaded from CHARMM-GUI as described in our previous work [8]. The peptide and water were then position restrained allowing the lipid molecules to equilibrate around the peptide leading to the closure of the pore. This was followed up by a release of the restraints on water molecules thus letting them equilibrate; finally the restraints on peptides were also released. After that the system was equilibrated for 50 ns.

To understand the dependence of melittin reorientation on melittin concentration we simulated a system containing 4 melittins and 128 lipids. We placed three more melittin molecules at the headgroup water interface and let them bind to the bilayer surface. While the three melittins were bound to the bilayer surface, the fourth melittin was reoriented, by pulling the center of mass of its pulling group. We used 15 windows, as it was done for the 1/128 system and one extra window at 1.4 nm, with a force constant of 1000 kJ/mol to increase sampling in this window. Initial structures for our sampling simulations were created in a manner similar to the simulations of a system with P/L = 1/128. Thus, three melittin molecules were first placed slightly above the bilayer with the pore and allowed to bind to the bilayer. After that another melittin at different orientations was added, and the equilibration steps were repeated, as was done for the 1/128 system.

II b) Regular MD simulations for the reorientation process: To get a better understanding of the peptide reorientation dynamics from parallel to the transmembrane conformation, we performed six regular MD simulations 200 ns in length each: three for the system with P/L = 1/128 and three for the P/L = 4/128 system. For initial configurations we selected the snapshots from the systems when the pulling group was around 1 nm, 0 nm and −1 nm from the bilayer center, at these distances the peptide is in parallel, intermediate and the perpendicular conformations.

Simulation details: The crystal structure of melittin was downloaded from the PDB databank (PDB ID: 2MLT) and the coordinates of chain A of the crystal structure were used to set up the system. The lipid bilayer consisted of 128 POPC lipids, 64 on each leaflet. All simulations were performed with the Gromacs package [14,15]: version 4.0.5. Melittin was described with the GROMOS96 force field [16] and the POPC lipids with the Berger force field parameters [17]. Melittin has a net charge of +6 since its N-terminus is protonated and hence 6 Cl^- ions were added to neutralize the systems. The water molecules were described by the SPC potential. All the systems were solvated in a 0.1 M NaCl solution, to resemble physiological conditions. The temperature was maintained at 310 K using the Nose–Hoover thermostat [18,19]. Pressure was maintained at 1 bar using semi-isotropic pressure coupling with the Parrinello–Rahman barostat [20]. The temperature and pressure coupling constants were set to 0.5 ps. The simulation time step was 2 fs. The Particle Mesh Ewald [21,22] method to calculate interactions for electrostatics, LINCS algorithm [23] to constrain covalent bond lengths and periodic boundary conditions were also used. The potentials of mean force (PMF) were obtained using the Weighted Histogram Analysis Method (WHAM) code implemented in the g_wham application of Gromacs [24,25]. The density and root mean square displacements were calculated using the g_density and g_rms scripts in GROMACS. The secondary structure analysis was performed using the DSSP module [26]. The PMFs were plotted using Xmgrace, the snapshots were visualized using VMD [27] and the 2D plots were visualized using MATLAB® (2011a).

3. Results and discussion

The presentation of our results follows the same sequence of topics as in the Methods section, where we described what performed.

I a): We estimated the free energy change and monitored the structural changes occurring to melittin during the process of its binding from water to the lipid bilayer surface, when the peptide approached the bilayer surface roughly in a parallel orientation. Fig. 1a displays the free energy change as a function of distance from the bilayer center. The gain in the free energy upon adsorption of melittin is −10.4 ± 1.7 kcal/mol, indicating a strong affinity of the peptide to the lipid bilayer, when it approached the bilayer parallel to its surface. (Following the procedure listed in [28,29] we calculated the free energy of peptide adsorption by integrating the PMF shown in Fig. 1a, and obtained a value of −10.66 ± 1.35 kcal/mol. The finite size effect described in [30] corrects this value by 0.27 ± 0.33 kcal/mol. Ladokhin and White [31] estimated that the free energy gain in a process when melittin transforms from an unfolded structure in water to a folded conformation on a POPC membrane surface is −7.6 kcal/mol. Given that we calculated the free energy under conformational restraints, our result is in a satisfactory agreement with the experimental estimate.) A large gain in free energy is, perhaps, caused by different factors, both energetic and entropic, including more energetically favorable interaction between molecules of the released water and gain in entropy due to its release. Detailed understanding of each factor requires a separate study, while for now we shall concentrate on the structural changes in the peptide. Thus, we considered the change in the RMSD of melittin, as it approached the bilayer (see Fig. 1b). Although each window calculation was started from the crystal structure, we only observed the unwinding of the helix at distances farther away from the bilayer. The helix structure was retained, as the peptide got closer to the bilayer. Melittin unfolded at distances above 3.3 nm while below this distance it adopted partially helical structures: around 2.5 nm melittin adopted a 73% helical structure. This is consistent with the experimental value of ~70% measured for melittin located on surfaces of POPC large unilamellar vesicles [3,31,32]. The plot of the RMSD as a function of distance also shows the flexible character of the peptide on the bilayer surface. The structural transformations of the peptide as a function of distance to the bilayer can also be seen from the snapshots i–iv in Fig. 1, which show that melittin becomes more folded, as it approaches the interface. The helical structure that we observe at 2.5 nm (Fig. 1-iv) remained stable for the last 100 ns and resembles the helical structure proposed for melittin located at the lipid interface by Hristova et al. [33]. They reported that the first 22 residues form an alpha-helix and

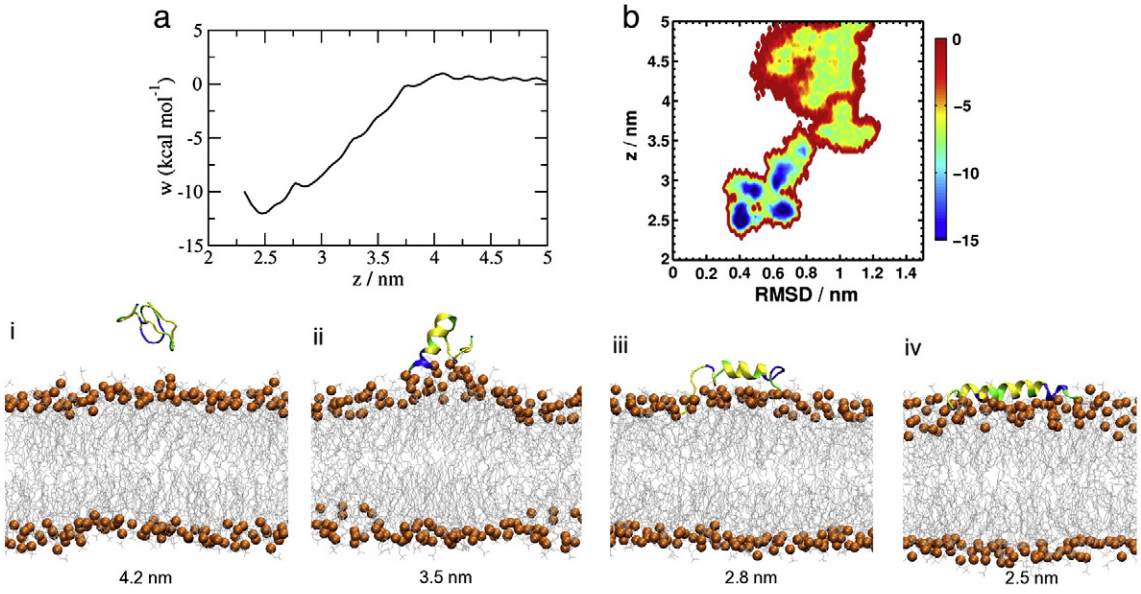

Fig. 1. a) PMF for pulling melittin in a parallel orientation to the bilayer from water to the bilayer surface. b) Change in the RMSD as a function of the distance from the bilayer center. The surface is colored by the PMF value. i–iv) Snapshots of melittin at different distances from the bilayer center. Phosphorous atoms are shown in orange and the lipid tails in gray, the peptide residues are colored by type: hydrophobic — yellow, hydrophilic — green and charged-blue.

the last four charged residues are extended along the helix axis. In our observations the first three residues are also extended as a coil.

I b): We placed two melittin peptides just outside of the lipid bilayer, one on each side. The hydrophilic residues of the peptide were facing the lipid headgroup atoms and hydrophobic residues faced water. The density distributions of the peptides, the time evolution of the distances between the center of mass of the peptide and the center of the bilayer and also the time evolution between the center of mass of the TRP residues and the center of the bilayer, along with the snapshots taken at 0, 100 and 200 ns are shown in Fig. 2. As we can see from the Figure, within the first 50 ns both peptides attached to the lipid bilayer. The peptide that got attached to the lower leaflet rotated around its helical axis and inserted into the bilayer, such that its TRP residue faced the lipid tails and the peptide assumed a shallow "U-shaped" conformation, which this peptide retained for the last 100 ns. As a result of peptide reorientation about its helical axis the hydrophilic side of the peptide now faced the headgroup region and the hydrophobic side faced the lipid tails. The average bending angle of the two helices (angle formed by the C-alpha atoms of residues 4, 14 and 26) was calculated to be 130° and 134° for the peptides attached to the upper and lower leaflets respectively. This is close to the bending angles of ~140° ± 24° or ~160° ± 24° obtained from NMR measurements performed on transmembrane oriented melittin in DMPC bilayers [34]. We observed that the TRP residue of the peptide attached to the upper leaflet underwent a constantly flapping motion, attempting to enter into the headgroup/tail interface. The described dynamics of the TRP residues from both peptides can be seen from Fig. 2-ii and 2-iii. The role of TRP in localizing the peptide on a lipid bilayer has also been under investigation [35].

Hristova et al. [33] determined the structure and the location of melittin in a DOPC bilayer using X-ray diffraction technique and found that the helical axis of melittin is located ~1.75 nm away from the bilayer center. Since one of our melittin peptides adopts a shallow "U-shape", we do not calculate the position of the helical axis. Instead we determine the distance of the center of mass of the two peptides from the center of the bilayer, as depicted in Fig. 2. Our results show that both melittin molecules remain located ~2 nm away from the bilayer center, which is consistent with observations of Hristova et al. Haldar et al. [36] also investigated properties of melittin in a DOPC bilayer by performing dansyl fluorescence experiments and they measured that the distance between the tryptophan residue and the center of the bilayer is ~1.06 nm. In our simulation, the average distance between the bilayer center and the TRP residue, belonging to the melittin in the lower leaflet of the POPC bilayer, is 1.27 nm, in the range of Haldar's observation. Notice that the thicknesses of pure DOPC and POPC bilayers are similar: 2.77 nm for DOPC and 2.71 nm for POPC [37,38].

II a): As we mentioned above, once adsorbed on the bilayer surface, melittin can spontaneously adopt a "U-shape" conformation, thus anchoring its termini to the polar headgroup region. Melittin peptides that adopt such "U-shaped" conformations were also observed in coarse-grained simulations, although the extent of bending was more significant in the coarse-grained simulations [12] which could be an effect of the force field or due to the large concentration of the peptides. During the simulations some of the peptides remained in the "U-shaped" conformations, but some reoriented into transmembrane conformation. To change from the "U-shaped" conformation to a transmembrane requires moving some of the charged residues across the membrane hydrophobic region. In order to understand the steps involved in the peptide reorientation and to understand the role of peptide concentration, we performed all-atom simulations with umbrella sampling, and pulled a group of atoms next to the N-terminus of melittin (see Methods section) from one leaflet of the bilayer towards the opposing leaflet. To study the melittin concentration effect on the reorientation, the pulling was performed for the P/L ratios of 1/128 and 4/128. Since the calculation of the free energy profile requires very extensive sampling of all possible conformations that can be achieved during a reorientation process, and it is very time consuming to perform, we did not calculate the potential of mean force. Instead, we focused on structural changes in the bilayer, in order to understand what makes the reorientation of the peptide possible.

We pulled the N-terminus and not the C-terminus across the bilayer because the C-terminus of melittin has a charge of +4 and the N-terminus has a charge of +1. Pulling the N-terminus across the hydrophobic core of the bilayer would induce much less perturbation

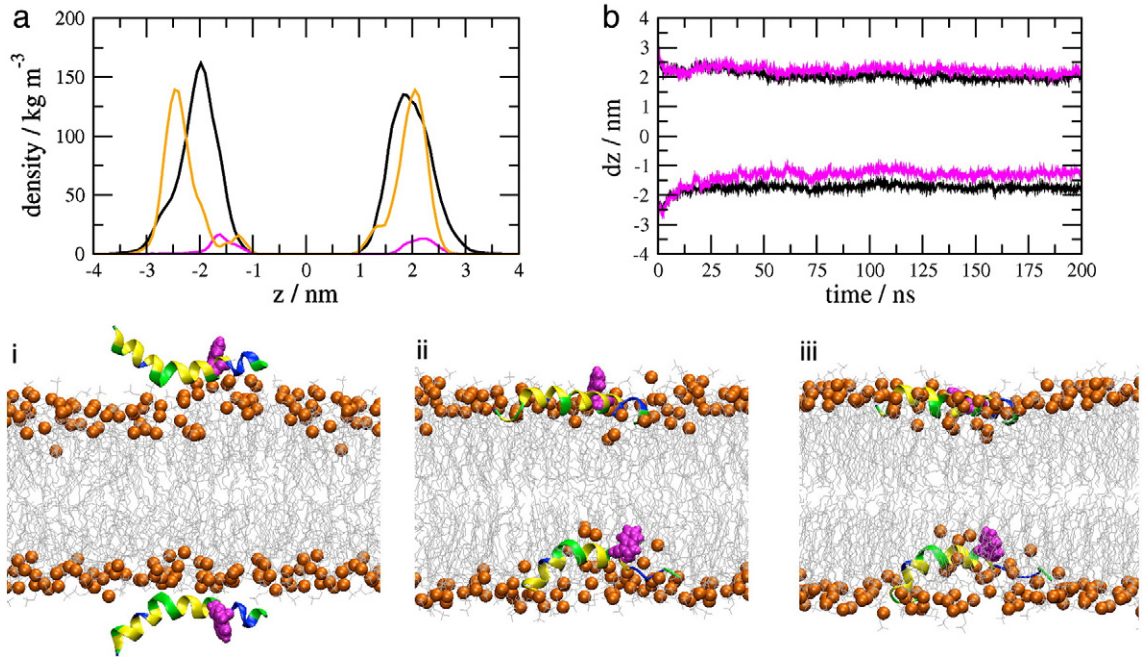

Fig. 2. a) Density distribution of the phosphorous atoms in the lipid (orange), peptides (black), and of TRP residues (magenta). All peptide atoms were included to get the density distribution shown in black, while only atoms belonging to the TRP residues were considered for the distribution shown in magenta. b) Position of the center of mass of the peptides (black) and the TRP residues (magenta). i–iii) Snapshots of the system at 0, 100 and 200 ns. The peptides are colored by the residue type, as in Fig. 1 with the TRP residues shown in VDW representation in magenta.

of the bilayer than pulling the C-terminus and, therefore, it requires less energy. Moreover, it was observed in a previous work that the C-terminus of melittin anchors to the headgroup atoms and the N-terminus tends to insert into the hydrophobic core [39,40]. We started our pulling simulations from a conformation similar to the one observed at the end of our regular MD simulations on melittin adsorbed on the bilayer surface.

Following up visually the trajectories during the pulling process we observed that as the N terminus of melittin was penetrating the hydrophobic region of the membrane, it was accompanied by some amount of water molecules. Thus defects in membranes filled up with water were created in the bilayer. In Fig. 3a we show 2-dimensional profiles for the water number density across the bilayer as a function of distance between the bilayer center of mass and the center of the pulling group (this distance is denoted as D) for the case P/L = 1/128. As the figure shows, the largest amount of water is present in the bilayer when the pulling group is close to the middle of the bilayer. At the same time we do not observe a continuous file of water across the bilayer. Water molecules follow the pulling group creating a water funnel between the pulling group and the closest lipid headgroup region. Fig. 3a shows that once the pulling group reaches the middle of the bilayer, the water funnel connecting the pulling group with the upper leaflet switches to a funnel connecting the pulling group with the lower leaflet. We made snapshots of the structures of the system while we pulled the peptide, and display some of these snapshots in the Fig. 3 i–iv. The snapshots show the switch of the funnels; while at D = 0.2 nm the funnel is between the pulling group and the upper bilayer, at D = −0.16 nm the funnel switched. Fig. 3b provides a similar information to the one presented in Fig. 3a, only for the case P/L = 4/128. From this figure it is clear that a pore filled out by water exists when the pulling group is located in the region when D has values between 0.1 nm and −0. 5 nm. This water pore is displayed in Fig. 3-vi and 3-vii for D = 0 nm and D = −0. 4 nm. Based on the behavior of water, as inferred from Fig. 3, it can be suggested that the transition region for the reorientation process for the case P/L = 1/128 is quite narrow and is located somewhere around D = 0.1 nm. For the case P/L = 4/128 the transition state is broad and occupies the region between D = 0.1 nm and D = −0.5 nm. From Fig. 3 we can also see that in addition to water penetrating the membrane, the headgroups of lipids next to peptide reorient, creating toroidal pores in the bilayer, as was observed in other simulations [5–7,9].

It should be noted that the lipid headgroups are not only pulled by the charged GLY1 residue, that is a part of the pulling group, but also by the LYS7 residue that is also charged. The long tail of the LYS7 allows it to snorkel and form salt bridges with the lipid headgroup atoms. As we can see in the snapshot iii of Fig. 3 at a distance around −0.16 nm the GLY1 interacts with the headgroup atoms of the lower leaflet causing bending of the lower leaflet while LYS7 interacts with the headgroup atoms in the upper leaflet leading to the bending of the upper leaflet. A similar behavior of the LYS residue was observed in the study of transportan 10 insertion into a POPC bilayer, where the LYS side chains were strongly associated with the headgroup atoms of the two leaflets during the insertion [41].

The snapshots at the transition region for D = 0 nm and D = −0.4 nm shown in Fig. 3-vi and 3-vii, resemble the pseudo-transmembrane conformation by Toraya et al. [42] using ^{31}P and ^{13}C-NMR spectroscopy and the rotational-echo double-resonance method. This pseudo transmembrane conformation has been used to build starting structures in computational simulations [7,9]. The snapshots in Fig. 3-vi and vii also resemble the disordered toroidal pores observed by Sengupta et al. [5] in their MD simulations performed for different P/L ratios of melittin. Our simulation indicates that a stable broad transition region exists for the case P/L = 4/128 characterized by penetrating water supporting a stable pore with a partially inserted peptide that is solvated by both water and reoriented lipid headgroups. The presence of such stable intermediates for the reorientation of melittin at higher P/L ratio can explain why simulation studies failed to observe a spontaneous peptide reorientation and also its transmission across the membrane.

II b): To better understand the character of the transition or near-transition regions we performed 200 ns runs of regular molecular dynamics simulations of systems with P/L = 1/128 and P/L = 4/128, starting with configurations shown in snapshots i, iii, iv, v, vii and viii of Fig. 3. For an easy visual comparison of the peptide conformational change we display snapshots of the initial configurations (which are the same as shown in Fig. 3) together with the snapshots of the corresponding final configurations in Fig. 4. We also show the trajectory of

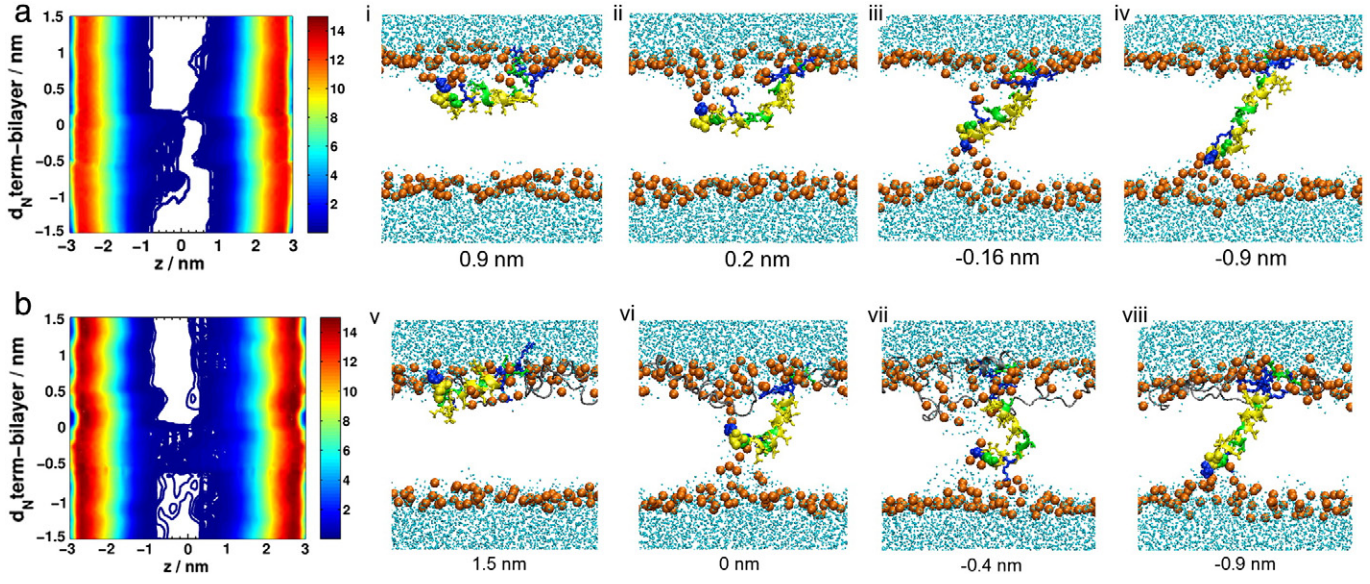

Fig. 3. a) Distribution of the number density of water as a function of the distance between the N-terminus residues and the center of mass of the bilayer for the system with the P/L ratio of 1/128. i–iv) Snapshots at different distances of the N-terminus from the bilayer center. The lipid tails are not shown for clarity, phosphorous atoms are shown as orange spheres, oxygen of water as blue spheres and the peptide is colored by the residue type as in Fig. 1 and the N-terminus residues being pulled are shown in a VDW representation. The residues of the protein are also shown in the stick representation to show their interaction with the bilayer and water as the peptide reorients. b) Distribution of the number density of water as a function of the distance between the N-terminus residues and the center of mass of the bilayer for the system with P/L ratio of 4/128. v–viii) Snapshots at different distances of the N-terminus from the bilayer center, the figure description is the same as for i–iv with the three extra peptides shown in gray.

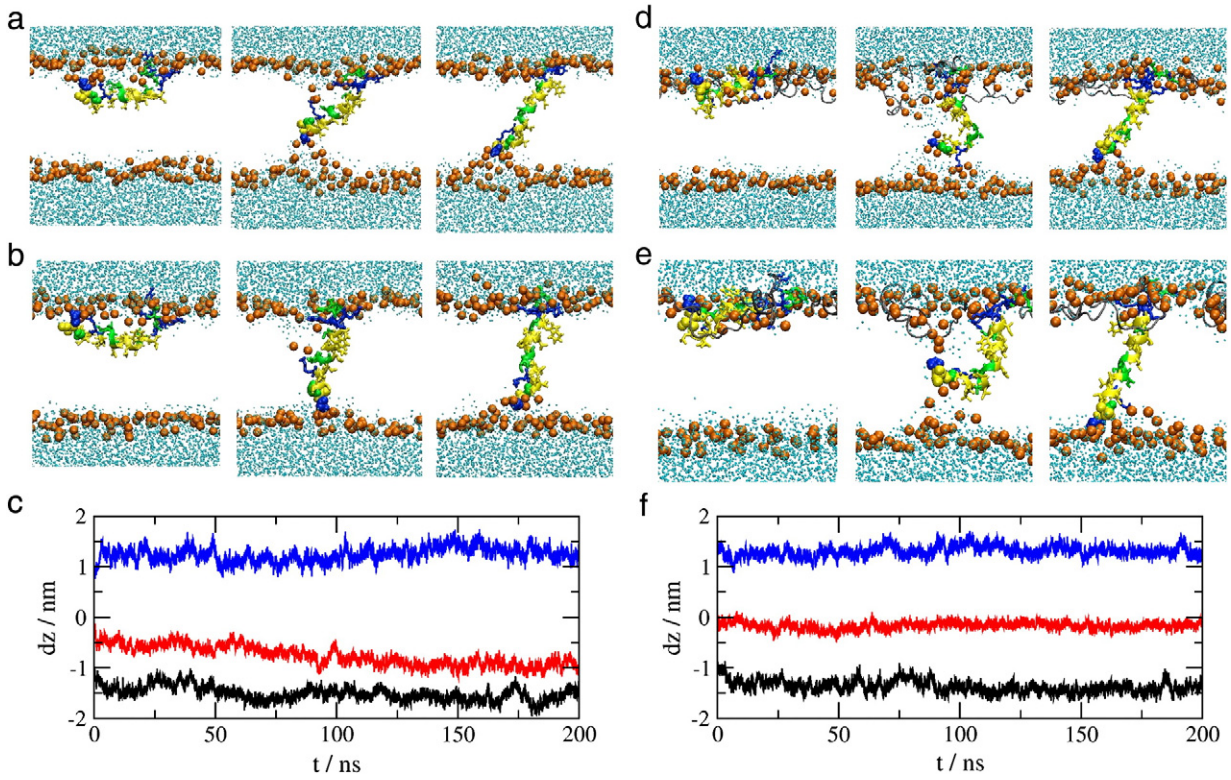

Fig. 4. a) Snapshots i, iii and iv from Fig. 3 for the system with P/L ratio of 1/128, that were used as starting structures for regular MD simulations. b) Snapshots of the system at the end of 200 ns regular MD. The color description is the same as in Fig. 3. c) distance between the center of mass of the first three residues of the N-terminus and the bilayer center of mass as a functions of time; blue for trajectory starting with snapshot i, red for snapshot iii and black for snapshot iv. d) Snapshots v, vii and viii from Fig. 3 for the system with P/L ratio of 4/128, that were used as starting structures for regular MD simulations. e) Snapshots of the system at the end of 200 ns regular MD. The color description is the same as in Fig. 3. f) Distance between the center of mass of the first three residues of the N-terminus and the bilayer center of mass as a functions of time; blue for trajectory starting with snapshot v, red for snapshot vii and black for snapshot viii.

the center of mass of the pulling group as the function of time (Fig. 4c and f). Our choice of initial configurations was dictated by the following reasoning: configurations i and v from Fig. 3 represent surface bound peptide, configurations iii and vii — pseudo-transmembrane and, finally, configurations iv and viii — transmembrane. From Fig. 4 we observe that surface bound and transmembrane conformations are stable for both P/L = 1/128 and P/L = 4/128 systems. For the run starting with pseudo-transmembrane conformations we observed that when P/L = 1/128, after 200 ns of MD the pseuo-transmembrane configuration transformed into fully transmembrane (see Fig. 4c). In case of P/L = 4/128 the pseudo-transmembrane conformation remained stable over 200 ns as shown in Fig. 4f. These observations are consistent with the observations we made above about the stability of the transition region.

4. Conclusions

The conformers of melittin as discussed in the literature [4] are: surface bound, transmembrane and pseudo-transmembrane, where the surface bound state is described as the conformation with the hydrophobic side of melittin facing lipid tails and the hydrophilic side facing headgroups. Such a structure is consistent with the description of the "U-shaped" structure we observe to occur spontaneously on melittin adsorption to the POPC bilayer surface. The pseudo-transmembrane conformation, where melittin inserts only partially into the hydrophobic core of the bilayer, resembles the conformations we observe for melittin in the 4/128 system, when the N-terminus is located around the center of the bilayer solvated by water and the headgroup atoms are in the pore. Melittin's preference for a parallel or perpendicular orientation has been proposed to depend on: a) concentration of melittin [43,44] — at low P/L ratios, melittin prefers a parallel orientation, as the P/L ratio increases the fraction of inserted peptides also increases. Chen et al. [45] used SFG and ATR-FTIR together and suggested that about three-fourths of melittin molecules orient parallel to the bilayer surface with a slight tilt and the rest have a perpendicular orientation. b) Degree of hydration of the model membrane [46] — in a hydrated membrane melittin prefers a parallel orientation and in a dry membrane it prefers a perpendicular orientation. c) Protonation of the N-terminus — if the N-terminus of melittin is protonated it prefers a perpendicular orientation [47]. d) Membrane potential (voltage dependence) [48] — a trans-negative voltage is required for the trans-membrane orientation of melittin. e) Hydrophobic length — Lazaridis et al. [49] observed that melittin's orientation depends on the thickness of the hydrophobic core of the lipid bilayer. To understand how all these factors determine the relative amount of parallel to membrane surface and transmembrane conformations we need to perform many detailed, labor extensive simulations. Our present simulations show, on a qualitative level, that with the increase of the peptide concentration resulting in a larger membrane tension, pores filled out with water, can be created and sustained. Presence of such pores may result in a lowering of a free energy barrier for the peptide reorientation and change the probability of different conformations.

Terwilliger et al. [50] proposed that melittin is a surface active peptide and its insertion into the membrane is unlikely because upon insertion the hydrophilic amino acids LYS7, THR10, THR11 and SER18 would be placed in a hydrophobic environment. However Vogel et al. [51] proposed that a transmembrane orientation for melittin is based on the possibility of a hydrogen bond between LYS7 and THR11 in the alpha-helical structure. This would significantly reduce the transfer free energy of LYS7 and create the possibility that upon association within the membrane melittin molecules could be oriented in such a way that their hydrophilic regions face each other. Peptide transfer is accompanied by creation of salt bridges with lipid headgroup atoms

or by direct solvation with water, factors that lead to water defects, explaining the insertion of peptides into lipid bilayers. More recent work focuses on water defects in the bilayer [52] that stabilize different orientations of melittin, which is consistent with our observations.

In summary: we have performed a systematic study to understand the binding and reorientation of melittin and to monitor the effect of increased peptide concentration. The process of binding takes place in two steps: adsorption of melittin to the lipid bilayer surface and rearrangement of melittin to adopt a shallow "U-shaped" conformation at the lipid bilayer headgroup/tail interface. The reorientation of melittin requires an increased peptide concentration, which induces membrane thinning facilitating pore formation that enables a reorientation of melittin into the transmembrane conformation.

Acknowledgements

This work was supported by the National Science Foundation under grant MCB-0950280. We thank Dr. Volker Knecht for active discussions and for suggesting the finite size correction. We also acknowledge the help of Dr. Jhuma Das and Mr. Tobias Pobandt at different stages of manuscript preparation.

References

[1] H.W. Huang, Molecular mechanism of antimicrobial peptides: the origin of cooperativity, Biochim. Biophys. Acta Biomembr. 1758 (9) (2006) 1292–1302.
[2] G. van den Bogaart, J.V. Guzman, J.T. Mika, B. Poolman, On the mechanism of pore formation by melittin, J. Biol. Chem. 283 (49) (2008) 33854.
[3] P.F. Almeida, A. Pokorny, Mechanisms of antimicrobial, cytolytic, and cell-penetrating peptides: from kinetics to thermodynamics, Biochemistry 48 (34) (2009) 8083–8093.
[4] H. Raghuraman, A. Chattopadhyay, Melittin: a membrane-active peptide with diverse functions, Biosci. Rep. 27 (4–5) (2007) 189–223.
[5] D. Sengupta, H. Leontiadou, A.E. Mark, S.J. Marrink, Toroidal pores formed by antimicrobial peptides show significant disorder, Biochim. Biophys. Acta Biomembr. 1778 (10) (2008) 2308–2317.
[6] M. Mihajlovic, T. Lazaridis, Antimicrobial peptides in toroidal and cylindrical pores, Biochim. Biophys. Acta 1798 (8) (2010) 1485–1493.
[7] M. Manna, C. Mukhopadhyay, Cause and effect of melittin-induced pore formation: a computational approach, Langmuir 25 (20) (2009) 12235–12242.
[8] S.J. Irudayam, M.L. Berkowitz, Influence of the arrangement and secondary structure of melittin peptides on the formation and stability of toroidal pores, Biochim. Biophys. Acta Biomembr. 1808 (2011) 2258–2266.
[9] J.H. Lin, A. Baumgaertner, Stability of a melittin pore in a lipid bilayer: a molecular dynamics study, Biophys. J. 78 (4) (2000) 1714–1724.
[10] S.J. Marrink, H.J. Risselada, S. Yefimov, D.P. Tieleman, A.H. De Vries, The MARTINI force field: coarse grained model for biomolecular simulations, J. Phys. Chem. B 111 (27) (2007) 7812–7824.
[11] A.J. Rzepiela, D. Sengupta, N. Goga, S.J. Marrink, Membrane poration by antimicrobial peptides combining atomistic and coarse-grained descriptions, Faraday Discuss. 144 (2010) 431–443.
[12] K. Santo, M.L. Berkowitz, The difference between Magainin-2 and Melittin assemblies in phosphatidylcholine bilayers: results from coarse-grained simulations, J. Phys. Chem. B 116 (9) (2012) 3021–3030.
[13] V. Vivcharuk, B. Tomberli, I.S. Tolokh, C.G. Gray, Prediction of binding free energy for adsorption of antimicrobial peptide lactoferricin B on a POPC membrane, Phys. Rev. E 77 (3) (2008) 031913.
[14] B. Hess, C. Kutzner, D. van der Spoel, E. Lindahl, Gromacs 4: algorithms for highly efficient, load-balanced, and scalable molecular simulation, J. Chem. Theory Comput. 4 (3) (2008) 435–447.
[15] D. van der Spoel, E. Lindahl, B. Hess, G. Groenhof, A.E. Mark, H.J.C. Berendsen, GROMACS: fast, flexible, and free, J. Comput. Chem. 26 (16) (2005) 1701–1718.
[16] W.F. van Gunsteren, S.R. Billeter, A.A. Eising, P.H. Hunenberger, P. Kruger, A.E. Mark, W.R.P. Scott, I.G. Tironi, Biomolecular Simulation: The GROMOS96 Manual and User Guide, 1996.
[17] O. Berger, O. Edholm, F. Jahnig, Molecular dynamics simulations of a fluid bilayer of dipalmitoylphosphatidylcholine at full hydration, constant pressure, and constant temperature, Biophys. J. 72 (5) (1997) 2002–2013.
[18] S. Nose, A unified formulation of the constant temperature molecular dynamics methods, J. Chem. Phys. 81 (1984) 511.
[19] W.G. Hoover, Canonical dynamics: equilibrium phase-space distributions, Phys. Rev. A 31 (3) (1985) 1695.
[20] M. Parrinello, A. Rahman, Polymorphic transitions in single crystals — a new molecular-dynamics method, J. Appl. Phys. 52 (12) (1981) 7182–7190.
[21] T. Darden, D. York, L. Pedersen, Particle mesh Ewald — an N.Log(N) method of Ewald sums in large systems, J. Chem. Phys. 98 (12) (1993) 10089–10092.
[22] U. Essmann, L. Perera, M.L. Berkowitz, T. Darden, H. Lee, L.G. Pedersen, A smooth particle mesh Ewald method, J. Chem. Phys. 103 (19) (1995) 8577–8593.
[23] B. Hess, H. Bekker, H.J.C. Berendsen, J.G.E.M. Fraaije, LINCS: a linear constraint solver for molecular simulations, J. Comput. Chem. 18 (12) (1997) 1463–1472.
[24] S. Kumar, J.M. Rosenberg, D. Bouzida, R.H. Swendsen, P.A. Kollman, The weighted histogram analysis method for free, energy calculations on biomolecules. I. The method, J. Comput. Chem. 13 (8) (1992) 1011–1021.
[25] J.S. Hub, B.L. de Groot, D. van der Spoel, g_wham — a free weighted histogram analysis implementation including robust error and autocorrelation estimates, J. Chem. Theory Comput. (2010).
[26] W. Kabsch, C. Sander, Dictionary of protein secondary structure: pattern recognition of hydrogen-bonded and geometrical features, Biopolymers 22 (12) (1983) 2577–2637.
[27] W. Humphrey, A. Dalke, K. Schulten, VMD: visual molecular dynamics, J. Mol. Graph. 14 (1) (1996) 33–38.
[28] H.S. Ashbaugh, B.A. Pethica, Alkane adsorption at the water-vapor interface, Langmuir 19 (18) (2003) 7638–7645.
[29] S.N. Jamadagni, R. Godawat, S. Garde, How surface wettability affects the binding, folding, and dynamics of hydrophobic polymers at interfaces, Langmuir 25 (22) (2009) 13092–13099.
[30] C.I.E. von Deuster, V. Knecht, Antimicrobial selectivity based on zwitterionic lipids and underlying balance of interactions, Biochim. Biophys. Acta Biomembr. 1818 (2012) 2192–2201.
[31] A.S. Ladokhin, S.H. White, Folding of amphipathic alpha-helices on membranes: energetics of helix formation by melittin, J. Mol. Biol. 285 (4) (1999) 1363–1369.
[32] A.S. Ladokhin, M. Fernandez-Vidal, S.H. White, CD spectroscopy of peptides and proteins bound to large unilamellar vesicles, J. Membr. Biol. 236 (3) (2010) 247–253.
[33] K. Hristova, C.E. Dempsey, S.H. White, Structure, location, and lipid perturbations of melittin at the membrane interface, Biophys. J. 80 (2) (2001) 801–811.
[34] A. Naito, T. Nagao, K. Norisada, T. Mizuno, S. Tuzi, H. Saito, Conformation and dynamics of melittin bound to magnetically oriented lipid bilayers by solid-state 31P and 13C NMR spectroscopy, Biophys. J. 78 (5) (2000) 2405–2417.
[35] A. Babakhani, A.A. Gorfe, J. Gullingsrud, J.E. Kim, J. Andrew McCammon, Peptide insertion, positioning, and stabilization in a membrane: insight from an all-atom molecular dynamics simulation, Biopolymers 85 (2007) 490–497.
[36] S. Haldar, H. Raghuraman, A. Chattopadhyay, Monitoring orientation and dynamics of membrane-bound melittin utilizing dansyl fluorescence, J. Phys. Chem. B 112 (44) (2008) 14075–14082.
[37] N. Kucerka, S. Tristram-Nagle, J.F. Nagle, Structure of fully hydrated fluid phase lipid bilayers with monounsaturated chains, J. Membr. Biol. 208 (3) (2006) 193–202.
[38] J. Pan, S. Tristram-Nagle, N. Kucerka, J.F. Nagle, Temperature dependence of structure, bending rigidity, and bilayer interactions of dioleoylphosphatidylcholine bilayers, Biophys. J. 94 (1) (2008) 117–124.
[39] A. Glattli, I. Chandrasekhar, W.F. Gunsteren, A molecular dynamics study of the bee venom melittin in aqueous solution, in methanol, and inserted in a phospholipid bilayer, Eur. Biophys. J. 35 (3) (2006) 255–267.
[40] S. Berneche, M. Nina, B. Roux, Molecular dynamics simulation of melittin in a dimyristoylphosphatidylcholine bilayer membrane, Biophys. J. 75 (4) (1998) 1603–1618.
[41] C.M. Dunkin, A. Pokorny, P.F. Almeida, H.S. Lee, Molecular dynamics studies of transportan 10 (Tp10) interacting with a POPC lipid bilayer, J. Phys. Chem. B (2010).
[42] S. Toraya, K. Nishimura, A. Naito, Dynamic structure of vesicle-bound melittin in a variety of lipid chain lengths by solid-state NMR, Biophys. J. 87 (5) (2004) 3323–3335.
[43] X. Chen, J. Wang, C.B. Kristalyn, Z. Chen, Real-time structural investigation of a lipid bilayer during its interaction with melittin using sum frequency generation vibrational spectroscopy, Biophys. J. 93 (3) (2007) 866–875.
[44] F.Y. Chen, M.T. Lee, H.W. Huang, Evidence for membrane thinning effect as the mechanism for peptide-induced pore formation, Biophys. J. 84 (6) (2003) 3751–3758.
[45] X. Chen, J. Wang, A.P. Boughton, C.B. Kristalyn, Z. Chen, Multiple orientation of melittin inside a single lipid bilayer determined by combined vibrational spectroscopic studies, J. Am. Chem. Soc. 129 (5) (2007) 1420–1427.
[46] S. Frey, L.K. Tamm, Orientation of melittin in phospholipid bilayers. A polarized attenuated total reflection infrared study, Biophys. J. 60 (4) (1991) 922–930.
[47] J.P. Bradshaw, C.E. Dempsey, A. Watts, A combined X-ray and neutron-diffraction study of selectively deuterated melittin in phospholipid-bilayers — effect of pH, Mol. Membr. Biol. 11 (2) (1994) 79–86.
[48] C. Kempf, R. Klausner, J. Weinstein, J. Van Renswoude, M. Pincus, R. Blumenthal, Voltage-dependent trans-bilayer orientation of melittin, J. Biol. Chem. 257 (5) (1982) 2469.
[49] T. Lazaridis, Effective energy function for proteins in lipid membranes, Proteins Struct. Funct. Bioinformatics 52 (2) (2003) 176–192.
[50] T.C. Terwilliger, L. Weissman, D. Eisenberg, The structure of melittin in the form I crystals and its implication for melittin's lytic and surface activities, Biophys. J. 37 (1) (1982) 353–361.
[51] H. Vogel, F. Jahnig, V. Hoffmann, J. Stumpel, The orientation of melittin in lipid membranes. A polarized infrared spectroscopy study, Biochim. Biophys. Acta Biomembr. 733 (2) (1983) 201–209.
[52] D. Parton, E. Akhmatskaya, M.S.P. Sansom, Multiscale simulations of the antimicrobial peptide maculatin 1.1: water permeation through disordered aggregates, J. Phys. Chem. B (2012).